Experimental realization of the Ehrenberg-Siday thought experiment

Giulio Pozzi, Chris B. Boothroyd, Amir H. Tavabi, Emrah Yücelen, Rafal E. Dunin-Borkowski, Stefano Frabboni, and Gian Carlo Gazzadi

Citation: Applied Physics Letters **108**, 083108 (2016); doi: 10.1063/1.4942462
View online: http://dx.doi.org/10.1063/1.4942462
View Table of Contents: http://scitation.aip.org/content/aip/journal/apl/108/8?ver=pdfcov
Published by the AIP Publishing

Experimental realization of the Ehrenberg-Siday thought experiment

Giulio Pozzi,[1,2] Chris B. Boothroyd,[1] Amir H. Tavabi,[1] Emrah Yücelen,[3]
Rafal E. Dunin-Borkowski,[1] Stefano Frabboni,[4,5] and Gian Carlo Gazzadi[5]
[1]*Ernst Ruska-Centre for Microscopy and Spectroscopy with Electrons and Peter Grünberg Institute, Forschungszentrum Jülich, D-52425 Jülich, Germany*
[2]*Department of Physics and Astronomy, University of Bologna, Viale B. Pichat 6/2, Bologna 40127, Italy*
[3]*FEI Company, Achtseweg Noord 5, 5600 KA Eindhoven, The Netherlands*
[4]*Department FIM, University of Modena and Reggio Emilia, via G. Campi 213/a, Modena 41125, Italy*
[5]*CNR-Institute of Nanoscience-S3, Via G. Campi 213/a, Modena 41125, Italy*

(Received 9 December 2015; accepted 9 February 2016; published online 23 February 2016)

In 1949, at the end of a paper dedicated to the concept of the refractive index in electron optics, Ehrenberg and Siday noted that wave-optical effects will arise from an isolated magnetic field even when the rays themselves travel in magnetic-field-free space. They proposed a two-slit experiment, in which a magnetic flux is enclosed between interfering electron beams. Now, through access to modern nanotechnology tools, we used a focused ion beam to open two nanosized slits in a gold-coated silicon nitride membrane and focused electron beam induced deposition to fabricate a thin magnetic bar between the two slits. We then performed Fraunhofer experiments in a transmission electron microscope equipped with a field emission gun and a Lorentz lens. By tilting the specimen in the objective lens field of the electron microscope, the magnetization of the bar could be reversed and the corresponding change in the phase of the electron wave observed directly in the form of a shift in the interference fringe pattern. © *2016 AIP Publishing LLC*. [http://dx.doi.org/10.1063/1.4942462]

In 1949, Ehrenberg and Siday observed that the expression for the electron-optical refractive index contains the vector potential and not the magnetic field strength, concluding that "one might expect wave-optical phenomena to arise which are due to the presence of a magnetic field but not due to the magnetic field itself, i.e., which arise whilst the rays are in field-free regions only".[1] They proposed an arrangement, whereby an enclosed magnetic flux is placed between two interfering beams in a two-slit experiment and predicted that the presence of the flux should result in a detectable phase shift. This effect was rediscovered ten years later by Aharonov and Bohm[2] in the context of quantum mechanics and is considered to be of great importance as it is the first example of quantum gauge phenomena (see, e.g., a historical report by Hiley[3]). It also raised a lively controversy between theoreticians and experimentalists, which has been thoroughly reviewed by Olariu and Popescu.[4] The off-axis holography experiments on toroidal superconductors by Tonomura and co-workers[5] can be considered the last word of an experimental feat started by the pioneering experiment of Chambers.[6] A recent paper by Batelaan and Tonomura[7] initiated another debate about the attribution of credit,[8,9] confirming that the effect still stimulates and stirs the scientific community.

Here, we take advantage of our previous expertise in the realization of the Feynmann thought experiment using modern instrumentation,[10,11] in order to realize the Ehrenberg-Siday proposal in a transmission electron microscope (TEM). The experimental setup is shown schematically in Fig. 1. A point-like monochromatic electron source S is imaged onto a plane OP by a lens L. If two narrow slits, which are separated by distance d, are inserted after the lens, then a two-beam Fraunhofer interference pattern of spacing s is observed on the plane OP, with a zeroth order maximum on the symmetry plane. The spacing of the interference fringes is given by the expression

$$s = \frac{\lambda c}{d}, \tag{1}$$

where λ is the de Broglie wavelength of the electrons and the camera length c is the distance between the plane of the slits and the observation plane. Let us insert a constant magnetic flux Φ after the slits in the region of the geometrical shadow between them. This localized flux can be generated by a magnetic field oriented perpendicular to the plane of the figure, for example by an infinite coil or, equivalently, an infinite uniformly magnetized bar of constant cross section. In both cases, the field is zero in vacuum, apart from a negligible contribution arising from the closure field if the length of the coil or bar is finite. The phase difference between the two electron paths, which is given by the expression[1,2,4]

$$\Delta\varphi = -\frac{e}{\hbar}\Phi, \tag{2}$$

acts on the interference fringe system produced by the two slits but *not* on the diffraction envelope from each individual

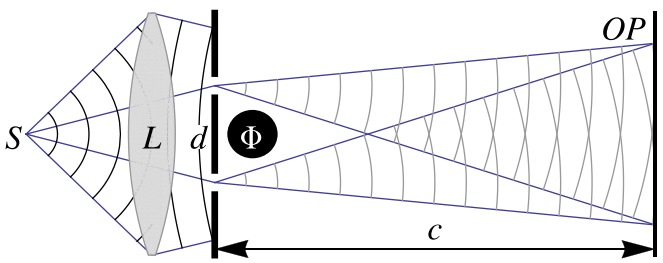

FIG. 1. Schematic diagram illustrating the basis of the Ehrenberg-Siday experiment, where an enclosed magnetic flux Φ is inserted between two slits in a two beam interference experiment.

slit.[4] The interference fringe system is displaced laterally with respect to the position for which $\Phi = 0$ by a distance Δx, which can be determined from the equation

$$\frac{\Delta x}{s} = -\frac{e}{\hbar}\Phi. \tag{3}$$

A phase difference of 2π results from the presence of flux $\Phi_0 = 2\pi\hbar/e = 4.135 \times 10^{-15}$ Wb. An intensity maximum is no longer observable in the symmetry plane unless $\Delta\varphi$ is a multiple of 2π. This result is gauge-independent, with the flux being related to the circulation of the vector potential. In order to observe this effect, which is easier to realize on a small scale using a magnetized bar than a coil, it is necessary to compare the results of experiments carried out for different values of magnetic flux. Taking advantage of modern nanotechnology techniques, we started by depositing Co bars in square patterned shapes on a C film (see Fig. 2). This process involves direct-write nanolithography and is based on the use of a focused electron beam to decompose gas precursor molecules (typically metallorganics) that have been adsorbed onto the substrate. Metal atoms are deposited onto the surface, while volatile ligands are pumped away after fragmentation of the molecules.[12]

The lateral dimensions of the patterns and the presence of a magnetic signature were initially confirmed using scanning electron microscopy (SEM), atomic force microscopy (AFM), and magnetic force microscopy (MFM) (see supplementary material).[13] As a result of the lack of purity of the deposited material, the saturation magnetization does not reach the value expected for bulk Co.[14] Moreover, it is difficult to measure its cross-sectional shape accurately. Several depositions were, therefore, performed, in order to obtain values of the enclosed magnetic flux that were suitable for the interference experiments.

We used Lorentz TEM to confirm that the Co rods were magnetized along their lengths by acquiring Fresnel defocus images at 200 kV using a conventional TEM (JEOL 2010). We tilted the specimen in the magnetic field of the weakly excited objective lens to observe changes in the asymmetry of the contrast of the Fresnel fringes at the edges of the rods. It was occasionally possible to observe the presence of a domain wall separating regions in the same Co rod that were magnetized in opposite directions. Such a domain wall can be seen in the lower part of Fig. 2.

Figure 3 shows simulations of Fresnel defocus images performed for an opaque magnetic bar of width 90 nm. In each image, there are two reversals in magnetization 2 μm apart. The four simulations correspond to phase shifts across the bar of $\pi/8$, $\pi/4$, $\pi/2$, and π. The defocus value used in the simulations is 15 mm.

In order to realize the Ehrenberg-Siday experiment, two slits were fabricated in a commercial silicon nitride membrane using a focused ion beam (FIB) workstation (FEI Strata DB 235 M). The sample consisted of a 3-mm-diameter, 200-μm-thick silicon frame, with a 100 μm $\times$ 100 μm square window at its centre. The entire sample was covered by a bi-layer comprising a 200-nm-thick silicon nitride membrane and a further 100-nm-thick Au film. The Au film was deposited onto the membrane before fabricating the slits. In order to create the slits, a 9 pA beam with a nominal spot size of 10 nm was scanned over two 30 nm $\times$ 480 nm boxes, spaced 500 nm apart, for 4 s for each box. The resulting slits were 48 nm wide, 490 nm apart, and 490 nm in length, as shown in Fig. 4.

The magnetic flux between the slits was provided by a Co nanorod, which was deposited between the slits using similar focused electron beam induced deposition (FEBID)[14] parameters to those used to fabricate the structure shown in Fig. 2. A Co carbonyl precursor $Co_2(CO)_8$ was used, and a 5 kV (110 pA) electron beam in an SEM was scanned across

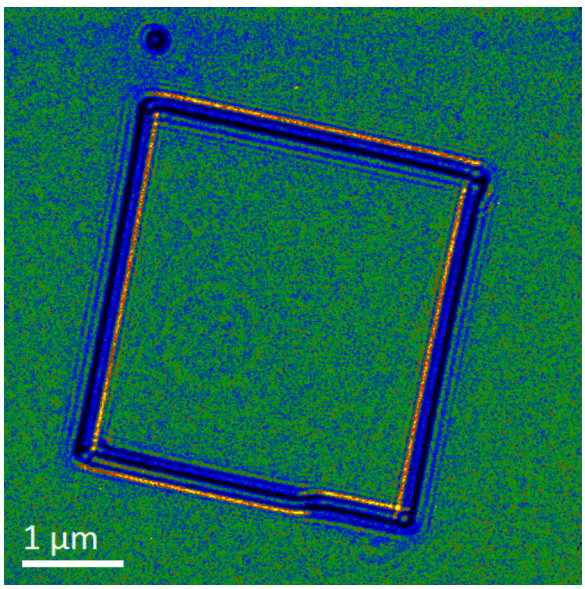

FIG. 2. Fresnel defocus image recorded in a transmission electron microscope showing the presence of a magnetic domain wall in one of the bars of a square patterned Co structure. The domain wall is visible as an abrupt change in the Fresnel fringes in the lower part of the square. Additional domain walls are present at three of the corners of the square.

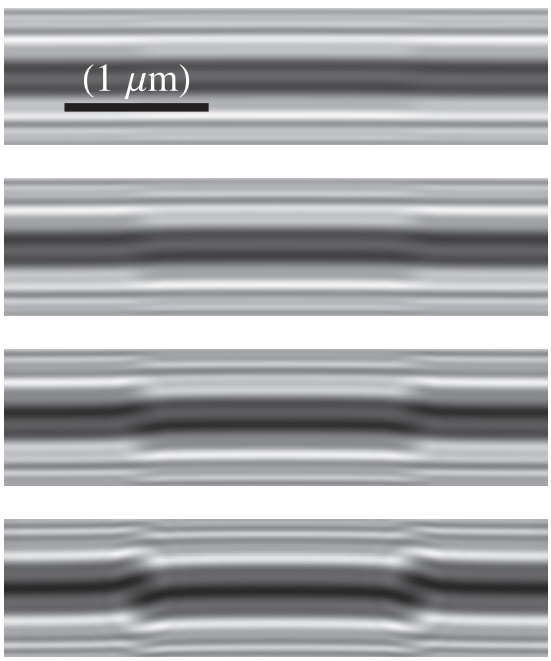

FIG. 3. Simulations of Fresnel defocus images of an opaque magnetic bar of width 90 nm at 15 mm defocus for an enclosed magnetic flux that results in a phase shift of $\pi/8$, $\pi/4$, $\pi/2$, and π from the top to the bottom.

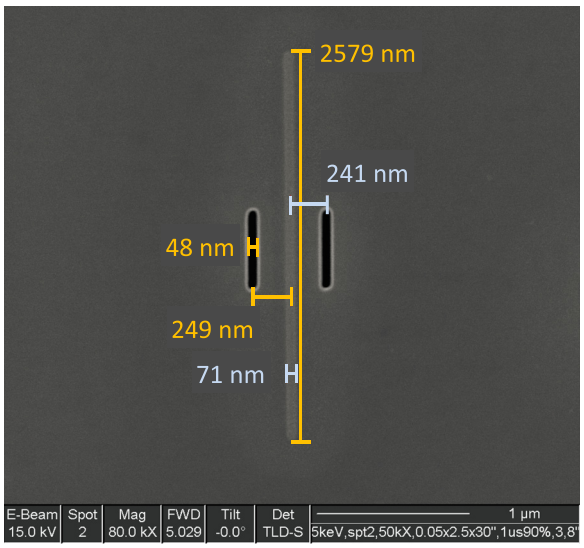

FIG. 4. SEM image of the two slits and Co nanorod. The Co nanorod is the vertical bar in the centre with length 2579 nm. The slits are the dark features on either side of the Co nanorod.

a 0.03 μm × 2.5 μm area under gas flow for 50 s, resulting in a 70-nm-wide, 50-nm-thick, and 2580-nm-long rod, as shown in Fig. 4.

Experiments aimed at demonstrating the Ehrenberg-Siday effect were carried out at 300 kV in an FEI Titan TEM equipped with a field emission gun, a Lorentz lens and a Gatan Imaging Filter (GIF). The specimen was inserted in the standard specimen plane, and its Fraunhofer diffraction pattern was recorded using (a) a camera length of 6.1 m on a standard charge-coupled device (CCD) camera located below the projection chamber of the microscope and (b)–(e) a camera length of 63 m on the GIF CCD camera, in order to highlight the broad central diffraction maximum modulated by interference fringes, as shown in Fig. 5.

The diffraction pattern shown in Fig. 5(a) was recorded with the specimen untilted in magnetic-field-free conditions. The presence of the magnetic flux is difficult to identify unless flux variations are introduced and differences between images are compared. Therefore, in a first series of experiments, a vertical magnetic field of 180 mT was applied by weakly exciting the objective lens of the microscope. The specimen was tilted about a horizontal axis lying in the specimen plane and perpendicular to the lengths of the slits and the bar. As visual observations carried out by manually tilting the specimen between ±20° indicated a jump in the interference fringes when the specimen tilt angle was approximately ±5°, a series of images was acquired at −2° (Fig. 5(b)), −4° (Fig. 5(c)), −6° (Fig. 5(d)), and −8° (Fig. 5(e)). Although there are small shifts in the position of the pattern, the images shown in (b) and (c) are clearly in registry, as are those in (d) and (e). A phase shift of approximately $\pm\pi/2$ can be seen between the patterns in (c) and (d), which is due to a reversal in the magnetization direction of the Co rod between the slits at a specimen tilt angle of approximately −5°. Intensity profiles generated from the Fraunhofer patterns in (c) and (d) are shown overlaid onto each other in Fig. 5(f) (−4° in blue and −6° in red).

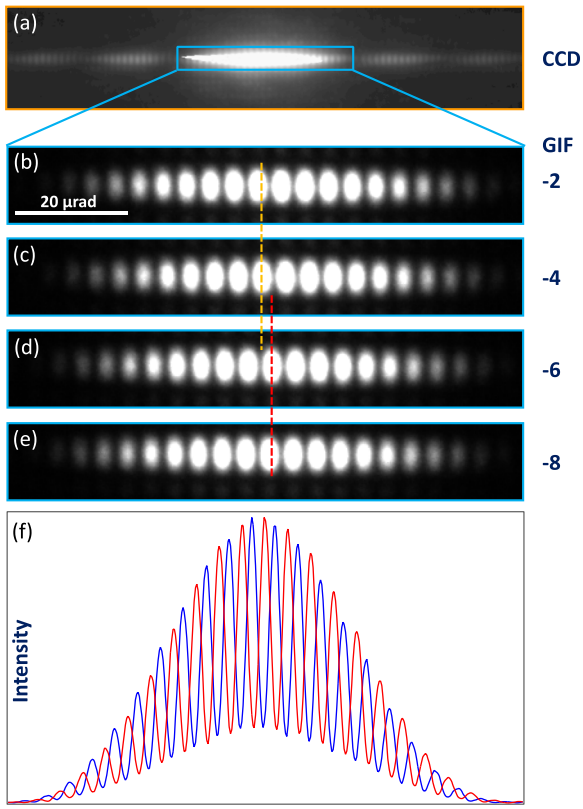

FIG. 5. (a) Low-angle electron diffraction image taken using a conventional (pre-GIF) CCD camera. (b)–(e) Low-angle electron diffraction images taken using a GIF CCD camera, recorded after tilting the sample between −2° and −8° in −2° steps. (f) Intensity line scans of (c) in blue and (d) in red.

A small but clear asymmetry in the interference pattern with a shift of the interference fringes with respect to the diffraction envelope can be observed, confirmed by the fact that the blue interference fringe maxima are higher than the red ones in the left part and lower in the right part of Fig. 5(f). This means that the two line scans cannot be overlapped by a rigid translation but are instead mirror symmetric and correspond to translations of the interference fringe system with respect to the diffraction envelope in opposite directions due to opposite magnetic phase shifts (see supplementary material).[13] Moreover, owing to the finite lateral partial coherence of the electron beam and the point spread function of the CCD camera, the minima do not reach a value of 0, as would be predicted for perfect coherence.

In order to obtain a more complete picture of the change in magnetization with specimen tilt angle, we also carried out dynamic experiments by recording images as the specimen tilt angle was varied continuously between ±20° (Multimedia view). Figure 6 shows the result of acquiring such a movie, separating it into individual frames, identifying the position and angle of the diffraction pattern in each frame, projecting the intensity parallel to the direction of the slits and placing the final one-dimensional line profiles above one another. Thus, in Fig. 6, the horizontal direction is the diffraction angle, while the vertical direction represents time and, therefore, also specimen tilt angle. From the top to the bottom of Fig. 6, there are two tilt cycles, in which the magnetization of the Co rod reverses twice.

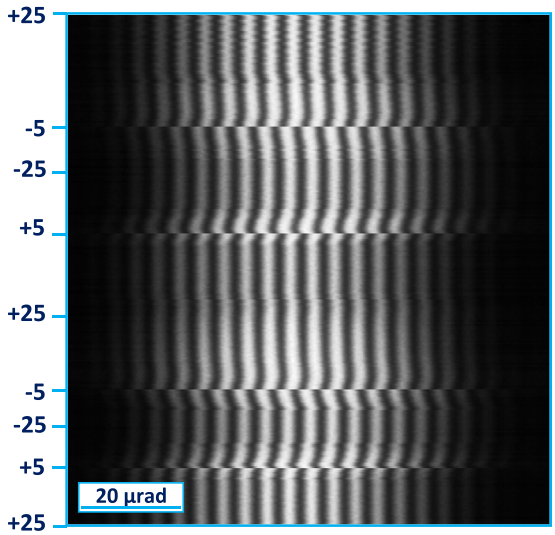

FIG. 6. Projected one-dimensional line profiles extracted from a movie of the interference pattern and displayed above each other from top to bottom, showing sideways shifts in the fringes and thus changes in the direction of magnetization in the Co rod during two tilting cycles between −25° and 25°. The vertical scale shows the approximate specimen tilt angle. As the actual tilt angle was not measured for each frame of the movie, this has been interpolated and is non-linear because the stage tilt rate was not constant. (Multimedia view) [URL: http://dx.doi.org/10.1063/1.4942462.1]

Although lateral shifts of the Fraunhofer images due to slight backlash in the specimen stage prevented their detailed comparison, it was possible to observe sudden movements of the fringes in correspondence with changes in magnetization of the Co rod. The fringe shift could be identified unambiguously, as the lateral shift and angular difference between consecutive frames is small. Moreover, analysis of the line scans across the transition (although poorer in quality when compared with standard images) shows the same behavior as in Fig. 5(f), confirming the shift of the interference fringes with respect to the diffraction envelope (see supplementary material).[13]

In conclusion, we have presented an experimental realization of the Ehrenberg-Siday proposal, which involves carrying out a two-slit electron interference experiment with a magnetic flux enclosed between the interfering electron beams. The experiment has been made possible by making use of modern nanotechnology and adds another important aspect to the Feynmann-Young two-slit experiment—that electromagnetic potentials are not simply useful mathematical tools but also have a physical meaning.[2,4]

We acknowledge Dr. F. Venturi (FIM) for his collaboration in the Lorentz Microscopy experiments and Dr. G. Lulli (IMM-CNR) for help with the multimedia. We are grateful to the European Union Seventh Framework Programme for funding under Grant Agreement 312483-ESTEEM2 (Integrated Infrastructure Initiative-I3) and to the European Research Council for an Advanced Grant No. 320832.

[1]W. Ehrenberg and R. E. Siday, "The refractive index in electron optics and the principles of dynamics," Proc. Phys. Soc., Sec. B **62**, 8–21 (1949).
[2]Y. Aharonov and D. Bohm, "Significance of electromagnetic potentials in the quantum theory," Phys. Rev. **115**, 485–491 (1959).
[3]B. Hiley, "The early history of the Aharonov-Bohm effect," preprint arXiv:1304.4736 (2013).
[4]S. Olariu and I. I. Popescu, "The quantum effects of electromagnetic fluxes," Rev. Mod. Phys. **57**, 339–436 (1985).
[5]A. Tonomura, N. Osakabe, T. Matsuda, T. Kawasaki, J. Endo, S. Yano, and H. Yamada, "Evidence for Aharonov-Bohm effect with magnetic field completely shielded from electron wave," Phys. Rev. Lett. **56**, 792 (1986).
[6]R. G. Chambers, "Shift of an electron interference pattern by enclosed magnetic flux," Phys. Rev. Lett. **5**, 3–5 (1960).
[7]H. Batelaan and A. Tonomura, "The Aharonov-Bohm effects: Variations on a subtle theme," Phys. Today **62**(9), 38–43 (2009).
[8]P. A. Sturrock, T. R. Groves, A. Ershkovich, C. A. Mead, H. Batelaan, and A. Tonomura, "More variations on Aharonov-Bohm," Phys. Today **63**(4), 8–9 (2010).
[9]M. Berry and M. Peshkin, "Aptly named Aharonov-Bohm effect has classical analogue, long history," Phys. Today **63**(8), 8–9 (2010).
[10]S. Frabboni, G. C. Gazzadi, and G. Pozzi, "Nanofabrication and the realization of Feynman's two-slit experiment," Appl. Phys. Lett. **93**, 073108 (2008).
[11]S. Frabboni, G. C. Gazzadi, and G. Pozzi, "Ion and electron beam nanofabrication of the which-way double-slit experiment in a transmission electron microscope," Appl. Phys. Lett. **97**, 263101 (2010).
[12]G. C. Gazzadi, H. Mulders, P. Trompenaars, A. Ghirri, M. Affronte, V. Grillo, and S. Frabboni, "Focused electron beam deposition of nanowires from cobalt tricarbonyl nitrosyl ($Co(Co)_3NO$) precursor," J. Phys. Chem. C **115**, 19606–19611 (2011).
[13]See supplementary material at http://dx.doi.org/10.1063/1.4942462 for additional experimental data, theoretical analysis and measurements.
[14]L. Serrano-Ramón, R. Córdoba, L. A. Rodríguez, C. Magén, E. Snoeck, C. Gatel, I. Serrano, M. R. Ibarra, and J. M. De Teresa, "Ultrasmall functional ferromagnetic nanostructures grown by focused electron-beam-induced deposition," ACS Nano **5**, 7781–7787 (2011).